AMERICAN SOCIETY FOR MICROBIOLOGY | Applied and Environmental Microbiology®

ENZYMOLOGY AND PROTEIN ENGINEERING

Biochemical Reconstruction of a Metabolic Pathway from a Marine Bacterium Reveals Its Mechanism of Pectin Depolymerization

Joanne K. Hobbs,[a] Andrew G. Hettle,[a] Chelsea Vickers,[a]* Alisdair B. Boraston[a]

[a]Department of Biochemistry and Microbiology, University of Victoria, Victoria, British Columbia, Canada

ABSTRACT Pectin is a complex uronic acid-containing polysaccharide typically found in plant cell walls, though forms of pectin are also found in marine diatoms and seagrasses. Genetic loci that target pectin have recently been identified in two phyla of marine bacteria. These loci appear to encode a pectin saccharification pathway that is distinct from the canonical pathway typically associated with phytopathogenic terrestrial bacteria. However, very few components of the marine pectin metabolism pathway have been experimentally validated. Here, we biochemically reconstructed the pectin saccharification pathway from a marine *Pseudoalteromonas* sp. *in vitro* and show that it results in the production of galacturonate and the key metabolic intermediate 5-keto-4-deoxyuronate (DKI). We demonstrate the sequential de-esterification and depolymerization of pectin into oligosaccharides and the synergistic action of glycoside hydrolases (GHs) to fully degrade these oligosaccharides into monosaccharides. Furthermore, we show that this pathway relies on enzymes belonging to GH family 105 to carry out the equivalent chemistry afforded by an exolytic polysaccharide lyase (PL) and KdgF in the canonical pectin pathway. Finally, we synthesize our findings into a model of marine pectin degradation and compare it with the canonical pathway. Our results underline the shifting view of pectin as a solely terrestrial polysaccharide and highlight the importance of marine pectin as a carbon source for suitably adapted marine heterotrophs. This alternate pathway has the potential to be exploited in the growing field of biofuel production from plant waste.

IMPORTANCE Marine polysaccharides, found in the cell walls of seaweeds and other marine macrophytes, represent a vast sink of photosynthetically fixed carbon. As such, their breakdown by marine microbes contributes significantly to global carbon cycling. Pectin is an abundant polysaccharide found in the cell walls of terrestrial plants, but it has recently been reported that some marine bacteria possess the genetic capacity to degrade it. In this study, we biochemically characterized seven key enzymes from a marine bacterium that, together, fully degrade the backbone of pectin into its constituent monosaccharides. Our findings highlight the importance of pectin as a marine carbon source available to bacteria that possess this pathway. The characterized enzymes also have the potential to be utilized in the production of biofuels from plant waste.

KEYWORDS glycoside hydrolase, pectin, polysaccharide lyase, zosterin, carbon metabolism, marine microbiology, pectic enzymes

Polysaccharides are abundant and chemically diverse macromolecules that are found in all ecological habitats. They represent an immense store of photosynthetically fixed carbon and source of energy to those organisms that possess the appropriate degradative and metabolic machinery to release it. Due to the complexity and chemical diversity of

Citation Hobbs JK, Hettle AG, Vickers C, Boraston AB. 2019. Biochemical reconstruction of a metabolic pathway from a marine bacterium reveals its mechanism of pectin depolymerization. Appl Environ Microbiol 85:e02114-18. https://doi.org/10.1128/AEM.02114-18.

Editor Volker Müller, Goethe University Frankfurt am Main

Address correspondence to Alisdair B. Boraston, boraston@uvic.ca.

* Present address: Chelsea Vickers, Faculty of Science, Thompson Rivers University, Kamloops, British Columbia, Canada.

Received 4 September 2018
Accepted 11 October 2018
Accepted manuscript posted online 19 October 2018
Published 13 December 2018

polysaccharides found in different environments, the carbohydrate-active enzymes (CAZymes), transporters, and other metabolic processing enzymes employed by heterotrophic organisms are usually specific for a particular polysaccharide and, therefore, ecological habitat (1). In bacteria, the genes encoding these specific proteins are often grouped together in the genome into coregulated regions known as polysaccharide utilization loci (PULs). These PULs define the metabolic capacity of the organism to utilize polysaccharides and thus greatly contribute to determining its environmental niche (2, 3).

Pectin is a complex and abundant family of polysaccharides found primarily in the cell walls of terrestrial plants (4). As such, its degradation and metabolism by microbes constitute an important component of the natural turnover of biomass, infection by plant pathogens, and digestion of dietary fiber in the mammalian gut (5–7). The simplest and most common pectin is homogalacturonan (HG), which comprises a linear backbone of α(1, 4)-linked D-galacturonate (GalUA) residues. These GalUA residues are commonly methylesterified at C-6 and are occasionally acetylesterified at O-2 or O-3 (8). Pectins can also contain more complex structural motifs, such as rhamnogalacturonan I (RGI) and rhamnogalacturonan II (RGII), which contain variable backbone structures and extensive side chain modifications. Given the abundance and structural nature of pectin in plant cell walls, a wide variety of microbes have acquired enzymatic pathways for the degradation and metabolism of this polysaccharide (5, 7, 9–13).

Because of its importance to phytopathogenesis, the metabolism of HG has been extensively studied over the last 50 years, allowing the construction of what we refer to as the canonical HG metabolism pathway, which is applicable to a wide variety of pectinolytic bacteria (13–18). Depolymerization is typically initiated extracellularly by one or more secreted *endo*-acting polysaccharide lyases (PLs), which cleave the HG backbone via a β-elimination mechanism, thereby generating oligouronates with 4,5-unsaturated nonreducing ends. Extracellular depolymerization is often assisted by other CAZymes, namely, carbohydrate esterases (CEs) and *endo*-acting α-galacturonidases belonging to glycoside hydrolase (GH) family 28. Saturated and unsaturated oligouronates then diffuse into the periplasm through porins belonging to the KdgM family. Once in the periplasm, oligouronates are further degraded into di- and trisaccharides by a different set of *endo*- and *exo*-acting PLs and an *exo*-acting GH28. Finally, these small oligogalacturonates are imported into the cytoplasm via the ATP-dependent transporter TogMNAB and degraded into saturated GalUA and Δ-4,5-unsaturated GalUA (ΔGalUA) by an intracellular oligogalacturonate lyase belonging to PL family 22 (13). In the cytoplasm, ΔGalUA undergoes KdgF-catalyzed linearization into 5-keto-4-deoxyuronate (DKI) (16) before it is further processed by an isomerase (KduI) and a reductase (KduD) into the key metabolite 2-keto-3-deoxygluconate (KDG) (19). GalUA is also converted into KDG by the actions of UxaC, UxaB, and UxaA, consecutively (20).

The discovery of GH105 enzymes, which are unsaturated uronyl hydrolases that cleave the 4,5-unsaturated residues from the nonreducing ends of PL-generated oligouronates (21, 22), has hinted at the potential for an alternate model of pectin metabolism. The mechanism of GH105 catalysis is thought to parallel that of GH88 members, which results in release of the linearized monosaccharide directly (23, 24). The direct release of DKI by GH105 enzymes would obviate the need for a PL22 (or potentially an equivalent) and KdgF to convert the unsaturated nonreducing ends of PL-generated oligouronates into DKI. The recent extensive characterization of complex pectin metabolism pathways in human gut microbiome *Bacteroides* spp. has suggested that GH105 enzymes would play a role in the complete saccharification of dietary pectin (7, 25).

Pectin is typically considered to be a terrestrial polysaccharide utilized by phytopathogens, plant cell wall-degrading saprophytes, and some members of the gut microbiome. However, the ability of some marine bacteria to grow on pectin and the secretion of pectin/pectate lyases by these organisms (26–30), as well as the recent identification of pectin-responsive PULs in a number of marine bacteria (29, 31), are shifting this view. These marine organisms are thought to target pectic substances found in marine diatoms and the cell walls of seagrasses (31–33). Zosterin, or marine

pectin, has been isolated and characterized from a number of species of seagrass belonging to the Zosteraceae family (33–36). It consists predominantly of apiogalacturonan (AGU), which is an HG backbone decorated with relatively frequent substitutions at O-3 of single residues, or short oligosaccharides, of D-apiose. RGI stretches, as well as methyl- and acetylesterification, have also been detected in zosterin (35). The marine *Bacteroidetes* member *Gramella flava* JLT2011 and the marine *Gammaproteobacteria* member *Pseudoalteromonas haloplanktis* ANT/505 both have the ability to degrade terrestrial pectin (27, 29). Proteomic and/or transcriptomic analysis has identified PULs within their genomes that are responsive to pectin and encode seemingly complete pectin degradation and catabolism pathways (29, 31). However, based on the genetic content of these PULs, these organisms appear to employ an enzymatic strategy for pectin degradation that differs from the canonical model (which relies on an arsenal of endo- and exolytic PLs and GH28s to fully degrade the HG backbone into GalUA and ΔGalUA and on KdgF to subsequently convert ΔGalUA into DKI). Rather, these marine microbes have genes encoding putative GH105 enzymes, and therefore it is anticipated, but not yet validated, that these organisms use a combination of PLs and GH105s to degrade HG to the key DKI intermediate.

We have previously isolated a marine species of *Pseudoalteromonas*, which we refer to as PS47, that is able to utilize multiple marine polysaccharides for growth (37). Here we report the identification and functional characterization of a pectin PUL from PS47 that shares regions of synteny and homology with those found in *G. flava* and *P. haloplanktis* ANT/505. Using the *Pseudoalteromonas* sp. strain PS47 pectin PUL as a model, we experimentally demonstrate the individual activities of seven key CAZymes from this marine pectin PUL. By biochemically reconstituting the complete enzymatic pathway *in vitro*, we show that together these enzymes degrade the HG backbone of pectin, liberating GalUA and DKI. Notably, the GH105 enzymes are demonstrated to play a critical role in the complete saccharification process, thus providing key biochemical support for the alternative pathway of pectin metabolism. On this basis, we propose a model of marine pectin degradation based on our experimental findings and discuss the presence of GH105s and an associated domain of unknown function among bacteria from distinct phyla.

RESULTS

***Pseudoalteromonas* sp. PS47 possesses a pectin utilization locus and produces pectinases.** *Pseudoalteromonas* sp. PS47 was isolated from the intertidal zone of Victoria, British Columbia, Canada, and found to grow on a number of marine polysaccharides. In agreement with this observation, CAZyme-specific annotation of its sequenced genome (with dbCAN2 [38] supplemented with manual curation) resulted in the identification of many genes encoding putative CAZymes targeted toward marine polysaccharides, including agarose, alginate, and carrageenan. On further analysis, we also identified an ~27,000-bp locus that includes a pair of genes encoding putative GH105 enzymes and likely genes encoding the metabolic machinery necessary to process both GalUA and DKI (Fig. 1A). This locus also encodes three putative CEs, a PL1 (putative pectin/pectate lyase), a GH28, a GH43 (putative β-xylosidase/arabinanase), a TonB-dependent transporter, and a tripartite ATP-independent periplasmic (TRAP) transporter. As expected, the transport and metabolic processing enzymes encoded in this locus are homologous to those encoded in the previously identified *P. haloplanktis* pectin PUL; however, based on the reported annotations, the CAZyme compositions in these two species initially appeared to be quite different (Table 1). Our reannotation of the *P. haloplanktis* PUL and sequence comparisons with proteins from the PS47 PUL actually revealed these two PULs to be very similar (Fig. 1A). The main points of difference are the addition of a multimodular PL1/CE8 and the reduction of a putative β-xylosidase/arabinanase into two cryptic genes in the *P. haloplanktis* PUL. The CAZyme annotation of the *G. flava* genome is publicly available through the Carbohydrate Active Enzymes database (www.cazy.org), and although the pectin PUL in *G. flava* PUL is more expansive in its CAZyme composition than the *Pseudoaltero-*

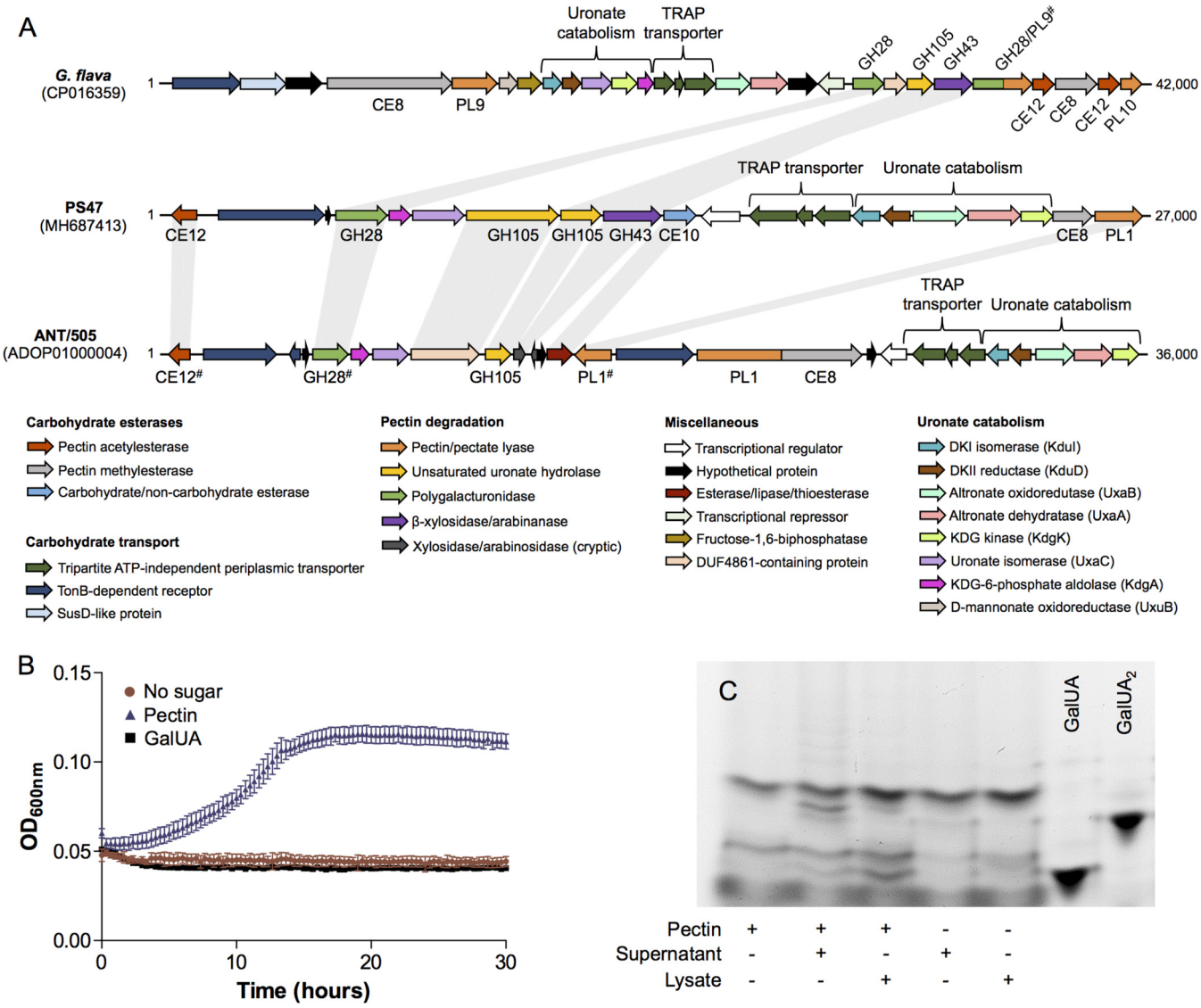

FIG 1 *Pseudoalteromonas* sp. PS47 contains a pectin utilization locus and produces pectinases. (A) Schematic depiction of the pectin utilization loci found in the genomes of *Gramella flava* JLT2011, *Pseudoalteromonas* sp. PS47, and *Pseudoalteromonas haloplanktis* ANT/505. Open reading frames (ORFs) are shown to scale (within a locus) and colored according to putative function. CAZyme family classifications, according to www.cazy.org and/or the dbCAN2 server, are given underneath or above; some of these classifications have been updated (indicated by #) and therefore differ from those originally reported by Tang et al. (29) and Hehemann et al. (31). Light gray bars between CAZyme-encoding ORFs indicate amino acid sequence identities of >40% (see Table 1 for exact sequence identities). Abbreviations: CE, carbohydrate esterase; GH, glycoside hydrolase; PL, polysaccharide lyase; DKI, 5-keto-4-deoxyuronate; DKII, 2,5-diketo-3-deoxygluconate; KDG, 2-keto-3-deoxygluconate. (B) Growth of PS47 on citrus pectin as the sole carbon source in minimal marine medium, with a no-sugar control shown for comparison. Absence of growth on galacturonate (GalUA) is also shown. Data shown are the mean of two biological replicates; error bars represent the SEM. (C) FACE gel showing the presence of pectinases in both the culture supernatant and cell lysate of PS47 grown in Zobell marine medium containing 0.2% pectin. + and −, presence and absence, respectively, of substrate or cell fraction. GalUA and digalacturonate ($GalUA_2$) were included on the gel as standards.

monas sp. PULs, the general complements of CAZyme functions are all similar (Fig. 1A and Table 1). Furthermore, all four GHs present in the *G. flava* PUL are homologous to one or more GHs from the PS47 PUL (Table 1). Given the genetic composition of the PS47 locus and its regions of homology and synteny with the *G. flava* and *P. haloplanktis* PULs, we hypothesized that the PS47 PUL also enables the degradation, uptake, and metabolism of marine pectin.

We initially addressed this hypothesis by investigating whether PS47 produced pectinases and could utilize pectin for growth. In general, growth of PS47 in minimal marine medium was limited, even on its preferred substrate (D-galactose) (data not shown), but it did exhibit some growth on citrus pectin (Fig. 1B). Interestingly, PS47 was

TABLE 1 Comparison of proteins present in pectin PULs from *Pseudoalteromonas* sp. PS47, *Pseudoalteromonas haloplanktis* ANT/505, and *Gramella flava* JLT2011

Protein name in PS47	dbCAN2 HMMER E value	Protein name in *P. haloplanktis* and locus tag[a]	% amino acid identity (PS47 vs *P. haloplanktis*)	Protein name in *G. flava* and locus tag[b]	% amino acid identity (PS47 vs *G. flava*)
*Ps*CE12	3.5e−72	RhgT (transcriptional regulator; GNTR)	63.5	Rga (CE12)	
		PH505_ap00680		GRFL_2179	5.6
				GRFL_218)	12.4
*Ps*GH28	1e−87	GhyB (amylomaltase; GH77)	75.3	PelL (GH28)	
		PH505_ap00640		GRFL_2174	46.0
				GRFL_2178	33.0
*Ps*GH105A	1.1e−106	DNA-directed RNA polymerase, α-subunit	64.5	RhiN (GH105)	38.4[d]
		PH505_ap00610		GRFL_2176	
*Ps*GH105B	4.2e−113	GhyA (GH105)	63.6	RhiN (GH105)	43.6
		PH505_ap00600		GRFL_2176	
*Ps*GH43	2.1e−71	XylA/B (xylosidase/arabinase)		XynB (GH43)	46.4
		PH505_ap00580	56.8[c]	GRFL_2177	
		PH505_ap00590	69.7[c]		
*Ps*CE10	5.9e−44	Esterase/lipase/thioesterase	52.8	NA[f]	NA
		PH505_ap00560			
*Ps*CE8	1.5e−31	PelA (pectate lyase/methylesterase; PL1; CE8)[e]	21.6[d]	PemA (CE8)	
		PH505_ap00520		GRFL_2158	5.4
				GRFL_2180	14.1
*Ps*PL1	9.5e−66	PelA (pectate lyase/methylesterase; PL1; CE8)[e]		NA	NA
		PH505_ap00520	15.0[d]		
		PelC (pectate lyase; PL3)			
		PH505_ap00550	51.6		

[a]From reference 31.
[b]From reference 29.
[c]Sequence identity based upon only partial coverage, as XylA (118 residues) and XylB (76 residues) are encoded by cryptic genes.
[d]For fusion proteins or proteins with additional domains, the sequence identity shown applies only to the homologous domain, not the entire protein sequence.
[e]The annotation of this protein as a bifunctional pectate lyase/methylesterase has been experimentally validated.
[f]NA, not applicable.

unable to grow on GalUA. We also detected the presence of pectinases in the supernatant and cell lysate from a culture of PS47 grown in pectin-supplemented Zobell broth by fluorophore-assisted carbohydrate electrophoresis (FACE) (Fig. 1C). A faint ladder of large labeled oligosaccharides and a strong band corresponding to approximately a disaccharide were visible following exposure of pectin to PS47 culture supernatant. Treatment of pectin with cell lysate produced smaller labeled products, including a band that likely corresponds to GalUA.

***Ps*PL1 is an endolytic pectate lyase active on a range of pectin-related substrates.** Having confirmed the presence of pectinase activity in cultures of PS47, we set out to biochemically identify and characterize the CAZymes responsible for this activity. Degradation of the HG backbone of pectin is typically initiated by a calcium-dependent endolytic PL; therefore, we cloned the putative PL1 encoded by the PS47 pectin PUL (*Ps*PL1) without its signal peptide, expressed it in *Escherichia coli*, and tested it for activity against a range of GalUA-containing substrates by FACE (Fig. 2A). *Ps*PL1 produced a faint ladder of oligosaccharides from citrus pectin and RGI, whereas it exhibited more extensive degradation of polygalacturonate (PGA) and AGU. In particular, *Ps*PL1 appeared to produce predominantly unsaturated digalacturonate (ΔGalUA-GalUA [$\Delta GalUA_2$]) from PGA. The high rate of production of oligouronates bearing a 4,5-double bond from PGA by *Ps*PL1 was also observed as an increase in absorbance at 230 nm (data not shown). The increased activity of *Ps*PL1 against PGA compared with pectin suggests that it is hindered by the decorations found on pectin and is therefore a pectate, rather than a pectin, lyase. We also used the increase in absorbance at 230 nm against PGA to determine the pH optima of *Ps*PL1 ($\geq$9) (see Fig. S1 in the supplemental material).

In order to determine the minimum degree of polymerization (DP) of GalUA oligosaccharides required by *Ps*PL1 for activity and to assist in our characterization of downstream enzymes, we used *Ps*PL1 to generate a range of unsaturated oligogalac-

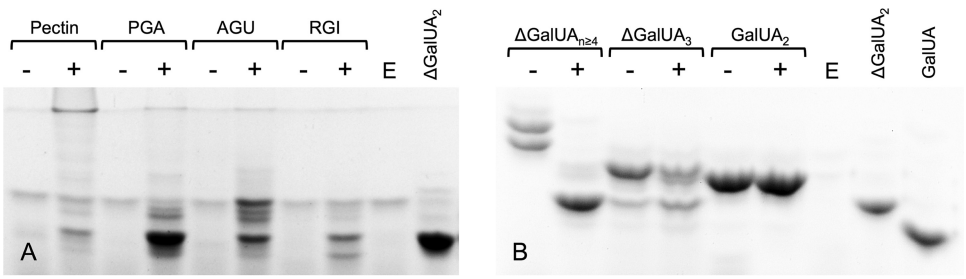

FIG 2 *Ps*PL1 displays endolytic lyase activity against a range of pectin-related substrates. (A) FACE gel of pectin and related polysaccharides following overnight incubation with 1 μM *Ps*PL1 in the presence of Ca^{2+}. + and −, presence and absence, respectively, of *Ps*PL1; E, enzyme-only sample. Abbreviations: PGA, polygalacturonate; AGU, apiogalacturonan; RGI, rhamnogalacturonan I; $\Delta GalUA_2$, unsaturated digalacturonate (included as a standard). (B) Activity of *Ps*PL1 against oligosaccharides of galacturonate with various degrees of polymerization. + and −, presence and absence, respectively, of *Ps*PL1; E, enzyme-only sample. $\Delta GalUA_2$ and galacturonate (GalUA) are included as standards.

turonates from PGA. *Ps*PL1 was incubated with PGA in the absence of calcium in an attempt to slow the degradation of larger oligosaccharides by *Ps*PL1 into $\Delta GalUA_2$ and obtain a panel of larger glycans. The resulting oligosaccharides were purified and their DPs estimated following comparison with standards labeled and separated by FACE (Fig. 2B). A relatively (~80%) pure unsaturated oligogalacturonate estimated to be unsaturated trigalacturonate (ΔGalUA-GalUA-GalUA [$\Delta GalUA_3$]) was obtained, as well as a mixture of larger unsaturated oligouronates with an estimated DP of ≥4. *Ps*PL1 was tested for activity against these purified glycans, in addition to $GalUA_2$, in the presence of calcium (Fig. 2B). *Ps*PL1 was able to completely degrade the larger oligosaccharides into $\Delta GalUA_2$, but activity against $\Delta GalUA_3$ was limited and $GalUA_2$ did not act as a substrate for *Ps*PL1. We suggest that these results are most consistent with *Ps*PL1 having endolytic pectate lyase activity with a minimum substrate DP requirement of 4.

Demethylation of pectin by *Ps*CE8 increases *Ps*PL1 activity. Our FACE results suggest that the activity of *Ps*PL1 is hindered by the esterification of citrus pectin. The PS47 pectin PUL encodes three putative CEs belonging to families 8, 10, and 12 (*Ps*CE8, *Ps*CE10, and *Ps*CE12). We cloned and expressed these three CAZymes without their signal peptides and tested them for pectin methyl- and acetylesterase activities using enzyme-coupled assays. These assays provide a read-out of liberated methanol and acetate, respectively. *Ps*CE8 exhibited methylesterase activity against pectin, while *Ps*CE12 demonstrated acetylesterase activity (Fig. 3A and B). *Ps*CE10 appeared to demonstrate both weak methyl- and acetylesterase activities, but only the acetyles-

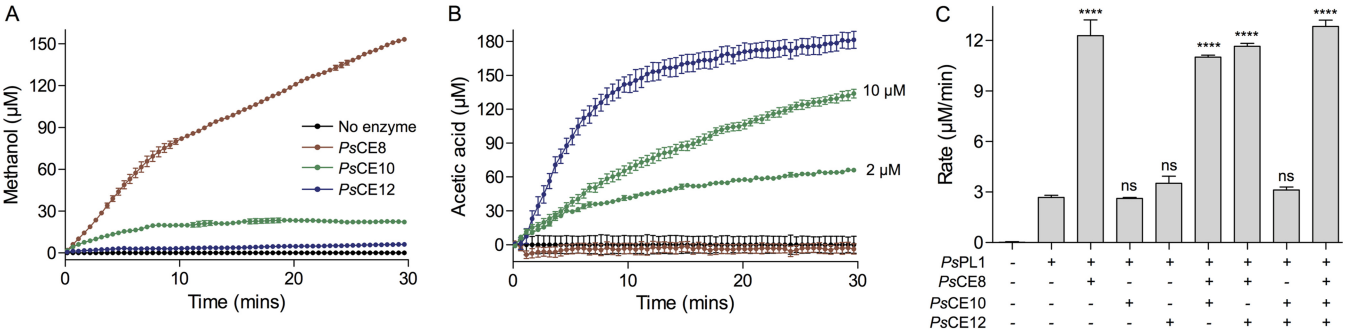

FIG 3 Terrestrial pectin is de-esterified by *Ps*CE8, *Ps*CE10, and *Ps*CE12. (A and B) The ability of the three putative pectin esterases to liberate methanol (A) or acetic acid (B) from citrus pectin was tested in enzyme-coupled assays. The weak acetylesterase activity of *Ps*CE8 was confirmed at two enzyme concentrations (2 μM and 10 μM); the apparent weak methylesterase activity of *Ps*CE10 seen in panel A was not increased in magnitude at 10 μM enzyme (data not shown), so it appears to be artifactual. The symbol legend applies to both panels. (C) The rate of unsaturated oligouronate production from pectin by *Ps*PL1 was monitored at 230 nm in the presence and absence of *Ps*CE8, *Ps*CE10, and *Ps*CE12 (indicated by + and −). Asterisks indicate statistically significant differences between enzyme combinations and the *Ps*PL1-only sample as determined by a one-way analysis of variance (ANOVA) with Bonferroni posttest (****, $P \leq 0.0001$; ns, $P > 0.05$). In all panels, data shown are the mean of three replicates and error bars represent the SEM.

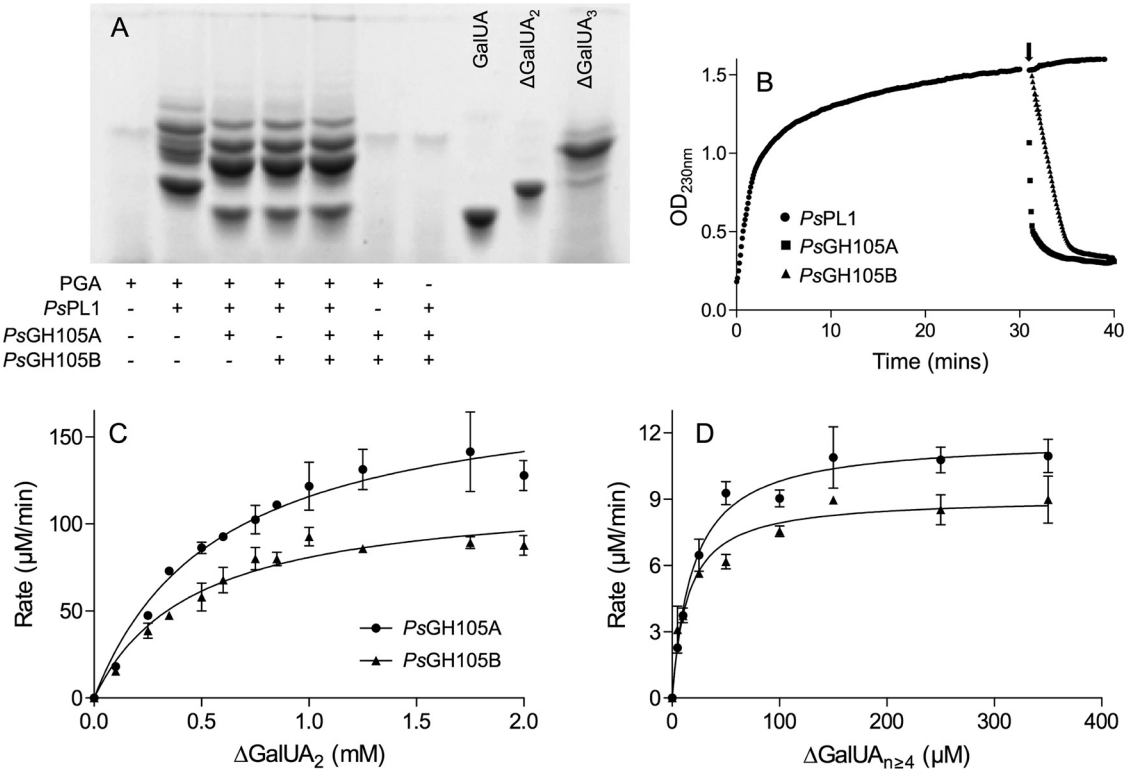

FIG 4 *Ps*GH105A and *Ps*GH105B act on the unsaturated oligogalacturonates produced by *Ps*PL1 with different efficiencies. (A) FACE gel showing the shift in the banding patterns of oligogalacturonates produced by *Ps*PL1 from polygalacturonate (PGA) following treatment with *Ps*GH105A, *Ps*GH105B, or both. Galacturonate (GalUA), unsaturated digalacturonate ($\Delta GalUA_2$), and unsaturated trigalacturonate ($\Delta GalUA_3$) were included as standards. + and −, presence and absence, respectively, of substrate or enzyme. (B) Removal of unsaturated uronyl residues from the nonreducing end of *Ps*PL1-generated oligogalacturonates by GH105As as detected by a decrease in OD_{230}. *Ps*PL1 was added to PGA in all reaction mixtures at time zero, and either *Ps*GH105A, *Ps*GH105B, or buffer was added to separate reaction mixtures after 30 min (indicated by the arrow). Data shown are the mean of three replicates, and error bars, where visible, represent the SEM. (C and D) Michaelis-Menten kinetics for *Ps*GH105A and *Ps*GH105B against $\Delta GalUA_2$ (C) and a mixture of unsaturated oligogalacturonates with an estimated degree of polymerization of ≥4 (D). Data shown are the mean of three replicates, and error bars represent the SEM. The enzyme concentrations used were 250 nM for both enzymes against $\Delta GalUA_2$ and 1 nM *Ps*GH105A and 10 nM *Ps*GH105B against $\Delta GalUA_{n\geq4}$.

terase activity was increased when the concentration of enzyme was increased; therefore, the apparent methylesterase activity is likely artifactual.

Given the presence of genes in the PUL encoding active esterases, we reasoned that their role would be to remove pectin modifications and thereby potentially aid depolymerization by *Ps*PL1. To test this, we measured the rate of 4,5-double bond production by *Ps*PL1 in the presence and absence of a single esterase or esterases in combination (Fig. 3C). Demethylation of pectin by *Ps*CE8 increased the rate of *Ps*PL1 activity by ~4-fold; deacetylation by *Ps*CE10 and/or *Ps*CE12 had no statistically significant effect. Despite the significant increase in rate observed in the presence of *Ps*CE8, the rate of *Ps*PL1 activity against pectin in the presence of *Ps*CE8 is still ~20-fold lower than that against unesterified PGA (data not shown).

PS47 possesses two Δ-4,5-unsaturated α-galacturonidases with different catalytic efficiencies. The action of *Ps*PL1 results in the production of small unsaturated oligogalacturonates. In pectin degradation pathways, these oligosaccharides can be further degraded by either exolytic pectate lyases or unsaturated galacturonyl hydrolases belonging to the GH105 family. As the PS47 pectin PUL encodes only a single PL (*Ps*PL1) but two GH105s (*Ps*GH105A and *Ps*GH105B), we cloned and expressed these two putative hydrolases and tested them for activity against the products of *Ps*PL1 (Fig. 4). PGA was treated with *Ps*PL1 in the absence of calcium so as to produce a ladder of products, the reactions were stopped by heating, and then the mixtures were split into aliquots to which the different GH105s (or no enzyme) were added (Fig. 4A). By FACE

analysis, we observed a shift down in the banding pattern produced by *Ps*PL1 together with either GH105 compared with *Ps*PL1 alone and also the appearance of a product migrating to the same point as the GalUA standard. While the unsaturated galacturonyl residue released by the GH105 would not be labeled by the fluorophore (due to its lack of a free aldehyde), cleavage of $\Delta GalUA_2$ by a GH105 would also result in the release of GalUA. The banding patterns produced by *Ps*GH105A and *Ps*GH105B, as well as both enzymes together, were not distinguishable from one another.

We also observed the activity of the GH105s on the products of *Ps*PL1 as a decrease in absorbance at 230 nm (Fig. 4B). This linked assay is essentially the same as we have previously used to demonstrate the double-bond depletion activity of KdgF (16). *Ps*PL1 was added to PGA, and the increase in absorbance at 230 nm was monitored for 30 min prior to the addition of *Ps*GH105A or *Ps*GH105B. In agreement with the FACE analysis, the addition of either GH105 resulted in an immediate and rapid decrease in absorbance. This rapid decrease in absorbance is consistent with removal of the terminal ΔGalUA and its direct conversion into DKI, which does not absorb at 230 nm; however, KdgF has previously been hypothesized to play a role in post-GH105 processing of oligouronates (31). We tested the effect of adding *Yersinia enterocolitica* KdgF (*Ye*KdgF), an enzyme that is known to catalyze the conversion of ΔGalUA to DKI (16), to our post-*Ps*PL1 reaction mixtures simultaneously with either GH105 and observed no alteration in the rate of double-bond depletion (data not shown). Therefore, the results support the direct release of the linear molecule DKI from unsaturated oligogalacturonides by *Ps*GH105A and *Ps*GH105B.

Our FACE analysis did not suggest any difference in substrate specificity between *Ps*GH105A and *Ps*GH105B; however, *Ps*GH105A did exhibit a higher rate of double-bond depletion than *Ps*GH105B against the pool of PGA-generated oligouronates (Fig. 4B). To further investigate this possible difference, we determined the Michaelis-Menten kinetics of both enzymes against $\Delta GalUA_2$ and $\Delta GalUA_{\geq n = 4}$ at their pH optima (pH 6.5 and 5.7 for *Ps*GH105A and *Ps*GH105B, respectively) (Fig. S1). The kinetics for *Ps*GH105A and *Ps*GH105B were very similar against $\Delta GalUA_2$ ($K_m = 0.58 \pm 0.1$ mM and 0.46 ± 0.1 mM, $k_{cat} = 12.2 \pm 0.9\ s^{-1}$ and $7.9 \pm 0.5\ s^{-1}$, and $k_{cat}/K_m = 21.0 \pm 3.9\ s^{-1}\,mM^{-1}$ and $17.2 \pm 3.9\ s^{-1}\,mM^{-1}$ for *Ps*GH105A and *Ps*GH105B, respectively [mean ± standard error of the mean {SEM}]), and both enzymes exhibited much higher affinities for the larger oligosaccharides ($21.2 \pm 3.7\ \mu M$ and $15.8 \pm 3.4\ \mu M$ for *Ps*GH105A and *Ps*GH105B, respectively) (Fig. 4C and D); however, the k_{cat} for *Ps*GH105A against $\Delta GalUA_{\geq n = 4}$ was >10-fold higher than that determined for *Ps*GH105B ($200.8 \pm 7.3\ s^{-1}$ versus $15.5 \pm 0.7\ s^{-1}$). These data indicate that both enzymes have considerably higher affinities for unsaturated oligogalacturonates larger than $\Delta GalUA_2$, but *Ps*GH105A is able to process these large glycans faster than *Ps*GH105B. As such, the catalytic efficiency (k_{cat}/K_m) of *Ps*GH105A against $\Delta GalUA_{\geq n = 4}$ is $9.5 \pm 1.7\ s^{-1}\,\mu M^{-1}$, compared with $1.0 \pm 0.2\ s^{-1}\,\mu M^{-1}$ for *Ps*GH105B.

Sequence analysis of *Ps*GH105A and *Ps*GH105B reveals that *Ps*GH105A is approximately twice the size of *Ps*GH105B due to the presence of an N-terminal domain of unknown function (DUF) belonging to family 4861. The DUF4861 family is uncharacterized, but its members are often found upstream of unsaturated uronyl hydrolases belonging to GH family 88 members. Therefore, it has been speculated that they may be involved in carbohydrate binding (http://pfam.xfam.org/family/PF16153). In order to test the potential carbohydrate binding function of the DUF of *Ps*GH105A and whether it contributes to the increased turnover rate of this enzyme compared with *Ps*GH105B, we cloned the DUF and catalytic domain of *Ps*GH105A separately. The boundaries for these constructs were determined based on domain annotations in BLAST (39) and dbCAN2 (38), a PHYRE2 homology model (40) of the catalytic domain, and secondary structure predictions for loop regions between the two domains (41–43). The DUF was successfully expressed and purified, and binding of this protein to PGA and $\Delta GalUA_{\geq n = 4}$ was evaluated using differential scanning fluorimetry (see Fig. S2 in the supplemental material). No change in the melting curve of the DUF was observed in the presence of either ligand at any concentration or pH. Unfortunately, the catalytic

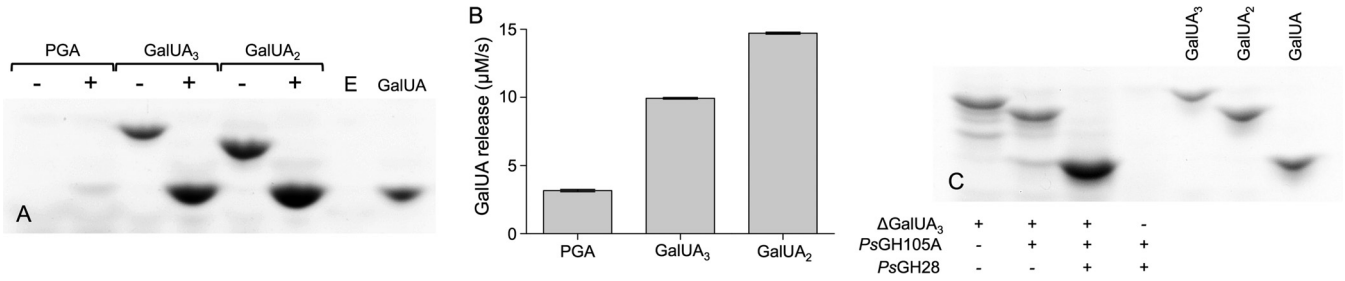

FIG 5 *Ps*GH28 is an *exo*-α-galacturonidase that liberates galacturonate from oligouronates. (A and B) Activity of *Ps*GH28 against polygalacturonate (PGA), trigalacturonate ($GalUA_3$), and digalacturonate ($GalUA_2$) as shown by FACE analysis (A) and turnover of released galacturonate by uronate dehydrogenase in an enzyme-coupled assay (B). + and −, presence and absence of *Ps*GH28, respectively; E, enzyme-only sample. Abbreviation: GalUA, galacturonate. Data shown in panel B are the mean initial rates from three replicates; error bars indicate the SEM. (C) FACE gel showing complete degradation of unsaturated trigalacturonate ($\Delta GalUA_3$) into GalUA by *Ps*GH105A and *Ps*GH28. $GalUA_3$, $GalUA_2$, and GalUA were included as standards. + and −, presence and absence of substrate or enzyme, respectively.

domain of *Ps*GH105A was expressed insolubly in *E. coli*; therefore, a comparison of catalytic parameters with and without the DUF could not be performed.

***Ps*GH28 is an *exo*-acting α-galacturonidase that completes the depolymerization of oligouronates.** The limited activity of *Ps*PL1 against oligogalacturonates with a DP of <4 hints toward a requirement by PS47 for an exolytic α-galacturonidase in order to fully utilize all the GalUA in the HG backbone of pectin. We cloned and expressed the GH28 encoded in the PS47 pectin PUL (*Ps*GH28) and investigated its activity against PGA and small saturated galacturonate oligosaccharides. FACE analysis showed that *Ps*GH28 released a small amount of a product with the same mobility as GalUA from PGA, and no detectable oligosaccharides, but was able to fully convert $GalUA_2$ and $GalUA_3$ into what appeared to be GalUA (Fig. 5A). To confirm the production of GalUA, we used an enzyme-linked assay in which a uronate dehydrogenase processes GalUA into D-galactarate with concomitant reduction of NAD^+. This revealed release of GalUA from PGA, $GalUA_2$, and $GalUA_3$ (Fig. 5B). *Ps*GH28 did not display any capability to degrade $\Delta GalUA_2$ (see Fig. S3 in the supplemental material), suggesting that *Ps*GH28 has strict *exo*-α-galacturonidase activity against saturated oligosaccharides.

The demonstrated *exo*-α-galacturonidase activity of *Ps*GH28 suggests that it would work synergistically with the GH105s to process the unsaturated oligogalacturonide products of *Ps*PL1, and we examined this by FACE. This analysis revealed that only cotreatment of $\Delta GalUA_3$ with *Ps*GH105A and *Ps*GH28 enabled complete depolymerization of the oligosaccharide, likely through the GH105-catalyzed release of $GalUA_2$ which is then a substrate for *Ps*GH28 (Fig. 5C). The same complete conversion of $\Delta GalUA_3$ into monosaccharides was also observed with *Ps*GH105B in place of *Ps*GH105A (data not shown).

PS47 enzymes work in concert to liberate GalUA and DKI. With its complement of CEs, GHs, and a PL, PS47 appears to possess all the enzymatic activities required to release both GalUA and DKI from pectin. We tested this theory by reconstituting the enzyme pathway *in vitro* and assessing the effect of omitting one or more enzymes on the rates of GalUA and DKI production. The rate of DKI production was measured as described previously (16) using a linked assay in which released DKI is processed by *Ye*KduI and *Ye*KduD into KDG with concomitant oxidation of NADH. The fully reconstituted enzyme pathway released significant amounts of both GalUA and DKI (Fig. 6). We also observed distinct differences in the importance of certain enzymes to the production of each monosaccharide. As expected, omission of both GH105s from the pathway completely abolished production of DKI, and *Ps*PL1 was also essential for DKI production, as it generates the unsaturated oligouronates upon which the GH105s act (Fig. 6A). Consistent with its isolated enzymatic activity, *Ps*GH28 had no significant effect on the DKI production rate but its omission had a profound effect on GalUA production. Exclusion of *Ps*PL1 and the two GH105s also had a significant effect on the rate of GalUA production (albeit not as pronounced as their effect on DKI release), as

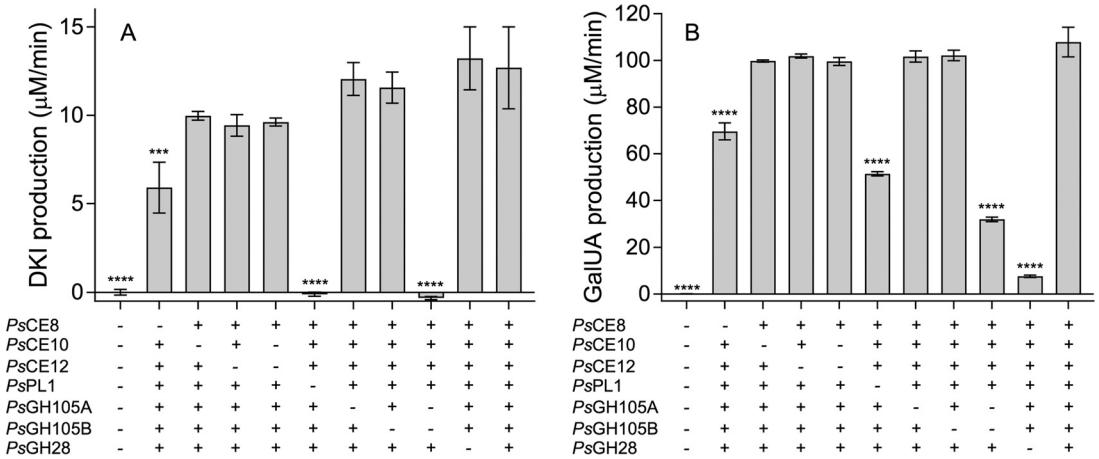

FIG 6 *In vitro* reconstitution of the pectin degradation pathway from *Pseudoalteromonas* sp. PS47. Linked assays in which the rates of DKI (A) and GalUA (B) production from pectin by PS47 enzymes were quantified by following their downstream processing into KDG (by *Ye*KduI and *Ye*KduD, with concomitant oxidation of NADH) and galactarate (by uronate dehydrogenase, with concomitant reduction of NAD^+), respectively, were performed. Data shown indicate the effect of omitting one or more enzyme. Data are the means of four replicates and have been corrected for background changes in absorbance in the presence of pectin only. Error bars represent the SEM. Asterisks indicate statistically significant differences between enzyme combinations and the "all enzymes" sample as determined by a one-way ANOVA with Dunnett's posttest (***, $P \leq 0.001$; ****, $P \leq 0.0001$; absence of asterisks, $P > 0.05$).

together these enzymes generate more saturated nonreducing ends for *Ps*GH28 to act on. In agreement with the observed effect of the esterases on the rate of *Ps*PL1 activity (Fig. 3C), only *Ps*CE8 had a significant effect on the production of either monosaccharide. We also observed redundancy among *Ps*GH105A and *Ps*GH105B, as omission of either one in isolation did not have a significant effect. In contrast, because the effect of excluding both acetylesterases was not significant, we were unable to distinguish whether *Ps*CE10 and *Ps*CE12 are redundant in their activities. Finally, we observed that addition of *Ye*KdgF to the reconstituted pathway did not increase the rate of DKI production (data not shown), thereby confirming the lack of a role for this enzyme in pectin degradation by PS47.

DISCUSSION

The classical pathway of pectin degradation and metabolism employed by terrestrial bacteria has been studied for more than 50 years, and its roles in biomass turnover and plant-pathogen interactions are well understood (14, 15, 44). Similarly, the presence of a pectin-like polysaccharide in marine seagrass was identified 50 years ago (33, 45). However, unlike in the case of terrestrial pectin metabolism, it was only recently that the capacity of marine bacteria to metabolize pectin was uncovered. Using the PS47 pectin PUL as a model, we have experimentally reconstructed an alternate pectin degradation pathway *in vitro* that utilizes a GH105 to carry out the equivalent chemistry typically afforded by an exolytic PL22 and KdgF in the canonical pathway used, for example, by bacterial phytopathogens (Fig. 7). The extracellular steps of the phytopathogen and marine pathways are essentially parallel, with de-esterification by CEs followed by backbone cleavage by an endolytic PL. The phytopathogen pathway also employs an endolytic GH28 to assist with backbone cleavage (this may be a function fulfilled by the apparent GH28/PL9 fusion encoded in the *G. flava* PUL). The resulting pool of small saturated and unsaturated oligogalacturonides is then imported into the periplasm for further degradation. In marine bacteria, this transport is likely carried out by a TonB-dependent receptor; these are transport proteins found in the outer membranes of Gram-negative bacteria and widely associated with carbohydrate utilization in marine microbes (46, 47). Once in the periplasm, marine bacteria employ one or more GH105s to remove the unsaturated galacturonyl residues and release DKI (and GalUA if the unsaturated substrate is a disaccharide) and an exolytic GH28 to cleave the

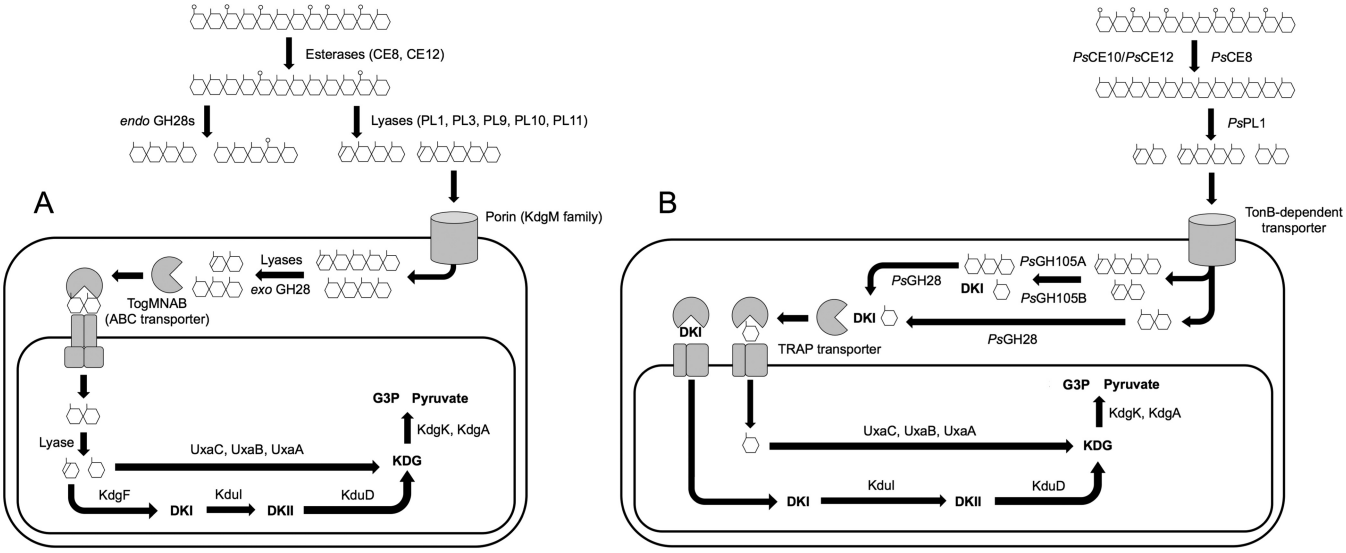

FIG 7 Comparison of the canonical pathway of pectin degradation and metabolism (A) and the pathway employed by *Pseudoalteromonas* sp. PS47 (B). Panel A is adapted from reference 17. Abbreviations: ABC, ATP binding cassette; TRAP, tripartite ATP-independent periplasmic; DKI, 5-keto-4-deoxyuronate; DKII, 2,5-diketo-3-deoxygluconate; KDG, 2-keto-3-deoxygluconate; G3P, glyceraldehyde-3-phosphate.

remaining saturated oligosaccharides into GalUA. Based on signal peptide and localization predictions (48, 49), we propose that *Ps*GH105A, *Ps*GH105B, and *Ps*GH28 are periplasmic and, therefore, that all monosaccharide production would occur in the periplasm. This is supported by the fact that PS47 is unable to grow on extracellular GalUA as the sole carbon source, indicating an inability to transport this monosaccharide (Fig. 1B). Import of the released GalUA and/or DKI from the periplasm into the cytoplasm is likely via the TRAP transporter that is encoded in all the known marine pectin PULs. Characterized TRAP transporters bind and transport a range of linear and cyclic acidic sugars, including GalUA (50, 51). We anticipate that the single TRAP transporter encoded in the PS47 pectin PUL may be able to import both GalUA and DKI into the cytoplasm, but this remains to be experimentally tested. In the canonical HG degradation pathway, a single transporter, TogMNAB, imports both saturated and unsaturated oligogalacturonides (52). These imported oligouronates are then further degraded by an exolytic PL (PL22), and KdgF linearizes the released ΔGalUA into DKI. The requirement for the PL22-KdgF pair is a key distinction between the phytopathogen and marine bacterial pectin degradation pathways. Finally, in both pathways, the intracellular processing of GalUA and DKI is catalyzed by an orthologous set of enzymes.

The PS47 PUL encodes two GH105 proteins with Δ-4,5-unsaturated α-galacturonidase activity. Homologs of these are also encoded in the *P. haloplanktis* and *G. flava* pectin PULs, though the functions of these enzymes have not been demonstrated (Table 1). Nevertheless, a hallmark of the marine pectin pathways studied to date is the presence of GH105-encoding genes, supporting the concept that utilizing a GH105 enzyme in a pectinolytic pathway avoids the requirement for an exolytic PL-KdgF pair.

The two GH105s, *Ps*GH105A and *Ps*GH105B, encoded in the PS47 pectin PUL each have homologs encoded in the *P. haloplanktis* PUL (Table 1). Based on the data presented here, *Ps*GH105A and *Ps*GH105B appear to be redundant in function. However, *Ps*GH105A possesses a DUF4861 and, with the data available, we were unable to evaluate whether the difference in catalytic efficiency between these two enzymes against longer oligouronates is due to the presence of DUF4861 or to variation within the GH105 domain itself. The *G. flava* pectin PUL encodes only a single GH105, which is not a fusion with a DUF4861; however, an adjacent gene encodes a putative protein that consists almost entirely of a DUF4861 (Fig. 1A). A GenBank search for DUF4861-containing proteins reveals that this domain is most commonly found as part of a larger

protein in *Proteobacteria*, such as *Pseudoalteromonas* spp., but exists as a stand-alone protein most often in *Bacteroidetes*. Therefore, this may represent an example of the fusion of protein functions among marine bacteria during the evolution of marine pectin degradation, as proposed by Hehemann et al. (31). Irrespective of whether they are partnered with another protein, DUF4861s are a common occurrence among pectin degradation PULs (see Fig. S4 in the supplemental material). Therefore, while the function of DUF4861 remains unknown, we can speculate that its presence is beneficial to efficient pectin catabolism in some way.

We have biochemically characterized seven key CAZymes from the PS47 PUL, and given the high amino acid sequence identity between these proteins and their homologs in *P. haloplanktis* ANT/505 (Table 1), we can infer that the *P. haloplanktis* PUL also encodes these activities. There remains one putative CAZyme from the PS47 PUL, *Ps*GH43, which we were unable to study due to its insoluble expression in *E. coli*. Characterized members of the GH43 family display β-xylosidase, α-arabinanase, and/or β-galactanase activity (www.cazy.org). As RGI fragments bearing xylose and arabinose side chains have been detected in zosterin (35, 53), it is reasonable to expect that the activity of *Ps*GH43 would be in line with its family classification. However, the presence of two cryptic genes for GH43s in the *P. haloplanktis* ANT/505 PUL, in place of the complete *Ps*GH43 gene found in PS47, may imply that a functional GH43 is not essential for marine pectin degradation. Other questions still remaining regarding the degradation of pectin by PS47 include the apparent absence of an apiosidase and inessentiality of the acetylesterases. Given that zosterin possesses a backbone of AGU, we would expect efficient marine pectin degradation to require an apiosidase. An endolytic apiosidase that is active on RGII was recently identified in *Bacteroides thetaiotaomicron* and represents the founding member of the new GH140 family (7). The PS47 genome does not encode any homologs of the *B. thetaiotaomicron* apiosidase; however, that does not mean that an apiosidase belonging to an as-yet-unidentified family is not present. In terms of the apparent lack of contribution of *Ps*CE8 and *Ps*CE10 to efficient pectin breakdown, this may be an effect of the pectin source used. The degree of acetylation of citrus pectin is reported to be $<$10% (54); therefore, the use of a pectin with more acetyl groups may reveal a more important role for these enzymes. Further investigation would also be required to determine whether *Ps*CE10 and *Ps*CE12 are redundant in function or whether they target acetyl groups attached to different oxygen atoms on GalUA.

In summary, we have reconstructed the complete biochemical pathway for pectin saccharification in a marine bacterium and demonstrated that it differs from the canonical pathway by its use of a GH105 and lack of a requirement for KdgF. Given the promise that microbes engineered to contain the canonical pectin degradation pathway have shown for the production of bioethanol from plant waste (55, 56), this alternate enzymatic pathway also has the potential to be exploited for the same purpose and may prove to be more efficient due to the requirement for fewer enzymes. In terms of the ecological niche occupied by PS47, this bacterium is capable of degrading alginate, agar, and carrageenan; therefore, it seems counterintuitive that it would acquire and maintain the capability to degrade pectin, a polysaccharide that has historically been considered terrestrial. Our experimental validation of the pectin degradation pathway employed by PS47 acts to highlight the importance of marine pectin as a carbon source for suitably adapted marine heterotrophs.

MATERIALS AND METHODS

Bacterial strains, plasmids, and materials. The isolation, genome sequencing, and annotation of *Pseudoalteromonas* sp. PS47 have been described previously (37). PS47 was routinely grown in Zobell marine broth or agar (HiMedia Laboratories, PA, USA) at 25°C. Polygalacturonic acid, citrus pectin, digalacturonic acid ($GalUA_2$), and trigalacturonic acid ($GalUA_3$) were purchased from Sigma-Aldrich (St. Louis, MO). Zosterin (apiogalacturonan) and rhamnogalacturonan I were obtained from Elicityl (Crolles, France) and Megazyme (Bray, Ireland), respectively. Unsaturated digalacturonate was a kind gift from Wade Abbott, Agriculture and Agri-Food Canada. All other reagents were from Sigma-Aldrich unless otherwise stated.

TABLE 2 Primers used in this study

Primer name	Primer sequence (5′→3′)[a]
*Ps*PL1 fwd	GCCGCGCGGCAGCCAACTCGACTCAAATTTAGCCTTTAAAAATGC
*Ps*PL1 rev	GCTCGAATTCGGATCGATTACTCCGTAATCGAATTTATATAAGC
*Ps*CE8 fwd	GCCGCGCGGCAGCCATTGCAACATCCACTCAAAAACACC
*Ps*CE8 rev	GCTCGAATTCGGATCTTATAAGCTAAAGCTATCAGTAGC
*Ps*CE10 fwd	GCCGCGCGGCAGCCAGAAAGAGTACACGTTGC
*Ps*CE10 rev	GCTCGAATTCGGATCTTATAGCTGTTTTTTTAAAAATAACG
*Ps*CE12 fwd	GCCGCGCGGCAGCCAGAAACAAGGTACAACACA
*Ps*CE12 rev	GCTCGAATTCGGATCTCAACCTTTTAGTTTTAAATGC
*Ps*GH105A fwd	GCCGCGCGGCAGCCAAAAAGAAAGCACTGCAGCAT
*Ps*GH105A rev	GCTCGAATTCGGATCTTACTTTACTGAGTTATCTATATC
*Ps*GH105B fwd	GCCGCGCGGCAGCCACGAGCCATTACCAAATAAAAATTTATG
*Ps*GH105B rev	GCTCGAATTCGGATCTTAACGCATCAAAGCAAGGCTAGC
*Ps*GH28 fwd	GCCGCGCGGCAGCCAATGTAAATCAGCCCCCCTTG
*Ps*GH28 rev	GCTCGAATTCGGATCTTACTGGGTTATTTTAGCTAA
*Ps*GH43 fwd	GCCGCGCGGCAGCCAAATGCGACCAATAAATATAATAATACTG
*Ps*GH43 rev	GCTCGAATTCGGATCTTAATTTTGCTCTGTTGGTGTGAAACG
*Ps*GH105A CAT fwd	GCCGCGCGGCAGCCAAGATGCAAAAAGTGCTTTAAAGTGG
*Ps*GH105A DUF rev	CTCGAATTCGGATCTTACAGTGGTGCTTTGAATTGAG

[a]Vector sequences used for In-Fusion cloning are underlined.

Growth of PS47 on pectin and detection of pectinase activity. Cells of PS47 grown overnight in Zobell marine broth were pelleted, washed, and diluted in complex minimal marine medium (57) containing no carbon source and then were used to inoculate 0.5 ml minimal medium containing either 1% (wt/vol) filtered citrus pectin, galactose, or no sugar in a 24-well tissue culture plate. One well for each carbon source was left uninoculated as a control. Plates were sealed with Breathe-Easy sealing membrane and incubated at 25°C in a SpectraMax M5 plate reader (Molecular Devices, San Jose, CA) for 60 h. Plates were shaken and readings of optical density at 600 nm (OD_{600}) taken every 20 min. OD readings were blanked against the absorbance of the uninoculated control well. For the detection of pectinases in cultures of PS47, the bacterium was grown overnight in Zobell marine broth plus 0.5% (wt/vol) citrus pectin at 25°C. A sample of culture was pelleted, the supernatant retained, and the pellet washed once with minimal marine medium containing no sugar before being resuspended in BugBuster plus DNase I. Following lysis at room temperature for 20 min, cellular debris was removed by centrifugation. Overnight digests (30 μl total) were set up containing 1.5% (wt/vol) citrus pectin in binding buffer (20 mM Tris-HCl [pH 8.0], 500 mM NaCl) with 5 μl of either culture supernatant or cleared lysate. Following digestion, reaction products were dried and labeled for fluorophore-assisted carbohydrate electrophoresis (FACE) as detailed below.

Cloning, protein expression, and purification. The genes encoding *Ps*PL1, *Ps*CE8, *Ps*CE10, *Ps*CE12, *Ps*GH43, *Ps*GH105A, *Ps*GH105B, and *Ps*GH28 were cloned, without any predicted signal peptides, into pET28a between the NdeI and BamHI sites using the In-Fusion HD cloning kit (Clontech Laboratories Inc., CA, USA) and the primers listed in Table 2. The cloning of *Ye*KdgF, *Ye*KduI, and *Ye*KduD has been reported previously (16). The catalytic domain and DUF4861 of *Ps*GH105A were also cloned separately into pET28a; the DUF construct consisted of residues 30 to 461 and the catalytic construct of residues 462 to 821. All cloning was confirmed by bidirectional sequencing (Sequetech Corp., CA, USA). Constructs were transformed into *Escherichia coli* BL21(DE3) for expression, and proteins were expressed in autoinduction medium at 16°C for 72 h or in Luria-Bertani broth with IPTG (isopropyl-β-D-thiogalactopyranoside) induction at 16°C for 18 h. Recombinant proteins were released from cells by chemical lysis and purified by immobilized Ni^{2+} affinity chromatography in binding buffer (20 mM Tris-HCl [pH 8.0], 500 mM NaCl) with an imidazole gradient. All proteins were assessed for purity by SDS-PAGE analysis, dialyzed against binding buffer overnight at 4°C, and concentrated using an Amicon stirred ultrafiltration unit fitted with either a 5- or 10-kDa-molecular-mass cutoff cellulose membrane, as appropriate, prior to use.

Production and purification of unsaturated galacturonate oligosaccharides. Polygalacturonate (1 g) was digested with 0.3 μM *Ps*PL1 in 20 mM Tris-HCl (pH 8.0) at 25°C and 70 rpm for 24 h. Any remaining full-length polysaccharide was removed by passing the digest through a 10-kDa-molecular-mass cutoff cellulose membrane using an Amicon stirred ultrafiltration unit. The flowthrough was lyophilized, resuspended in distilled water (dH_2O), and passed over a size exclusion column containing Bio-Gel P-2 (Bio-Rad, Hercules, CA) in 20 mM ammonium carbonate. Fractions containing unsaturated oligosaccharides were identified by measuring the absorbance at 230 nm in UV-Star 96-well microplates (Grenier Bio-One, Monroe, NC) in a SpectraMax M5 plate reader (Molecular Devices, San Jose, CA). Oligouronate size and separation were assessed by thin-layer chromatography as previously described (17). Any residual salts in fractions containing unsaturated oligouronates of a defined size were eliminated by repeating the size exclusion step with dH_2O before use.

FACE. Polysaccharide digests for fluorophore-assisted carbohydrate electrophoresis (FACE) analysis contained 0.5% (wt/vol) polysaccharide, 1 μM enzyme, and 1 mM $CaCl_2$ (when *Ps*PL1 was present) in binding buffer in 10-μl reaction mixtures and were incubated at 25°C overnight. Oligosaccharide digests were set up in the same way but contained approximately 10 μg substrate. All reaction products were dried, labeled with 20 mM 2-aminonaphthalene trisulfonic acid (ANTS), and separated in 35% polyacrylamide gels as previously described (58).

Esterase assays. All real-time enzyme assays were performed at 25°C in a SpectraMax M5 plate reader. *Ps*CE8, *Ps*CE10, and *Ps*CE12 were tested for acetylesterase activity using the Megazyme acetic acid assay kit according to the manufacturer's instructions. Reaction mixtures contained 0.3% (wt/vol) citrus pectin and 150 mM NaCl in kit buffer, and reactions were initiated by the addition of esterase to 2 or 10 μM. Data were processed according to the manufacturer's instructions and corrected for background changes in absorbance observed when binding buffer was added in place of esterase. Methylesterase activity was tested using an enzyme-coupled assay as described by Grsic-Rausch and Rausch (59). Reaction mixtures contained 0.2% (wt/vol) citrus pectin, 0.9 mM NAD^+, 1 U alcohol oxidase from *Pichia pastoris*, 0.02 U formaldehyde dehydrogenase from *Pseudomonas* sp., and 150 mM NaCl in 50 mM Tris (pH 7.5), and reactions were initiated by the addition of esterase to 5 or 10 μM. Data were corrected for background as described above and converted into concentrations of methanol using an extinction coefficient for NADH of 6,220 M^{-1} cm^{-1}. All statistical analyses were performed in GraphPad Prism 5 or 7.

Lyase assays. Lyase activity exhibited by *Ps*PL1 was observed in real time as an increase in OD_{230} in UV-Star 96-well microplates. The approximate pH optimum of *Ps*PL1 was initially determined using McIlvaine buffers (pH 4 to 8), and then the determination was repeated in 200 mM Tris-phosphate (pH 7 to 9). Reaction mixtures contained 0.1% (wt/vol) PGA and 1 mM $CaCl_2$, and reactions were initiated by the addition of *Ps*PL1 to 250 nM. The effect of the esterases on the rate of unsaturated oligogalacturonate production from pectin by *Ps*PL1 was determined in the presence of 0.3% (wt/vol) citrus pectin, 50 mM Tris (pH 8.0), and 150 mM NaCl. Reactions were initiated by simultaneous addition of *Ps*PL1 and esterase, each to a final concentration of 1 μM. Initial rates were converted into μM/min using an extinction coefficient for unsaturated uronates of 5,200 M^{-1} cm^{-1} as previously reported (6, 16).

Unsaturated galacturonyl hydrolase assays. Cleavage of unsaturated galacturonyl residues from the nonreducing end of oligogalacturonates by *Ps*GH105A and *Ps*GH105B was observed in real time as a decrease in OD_{230}. pH profiles were determined for *Ps*GH105A and *Ps*GH105B in McIlvaine buffers (pH 4 to 8) containing 1 mM $\Delta GalUA_2$ with 250 nM enzyme. The *Ps*PL1-*Ps*GH105 linked assay mixture contained 0.3% (wt/vol) PGA and 500 mM NaCl in 20 mM Tris (pH 8.0). *Ps*PL1 was added to 1 μM and the reaction was allowed to proceed for 30 min, at which point OD_{230} readings were paused for approximately 1 min to allow for the addition of either *Ps*GH105A or *Ps*GH105B to 200 nM. Michaelis-Menten kinetics were determined for *Ps*GH105A and *Ps*GH105B at their pH optima (pH 6.5 and 5.7, respectively) in 50 mM MES (morpholineethanesulfonic acid) buffer and 200 mM NaCl with 1 to 250 nM enzyme from initial rates in the presence of various concentrations of either $\Delta GalUA_2$ or a mixture of large unsaturated oligosaccharides with an estimated degree of polymerization of $\geq$4. The effect of *Ye*KdgF on the rate of unsaturated oligogalacturonate depletion by *Ps*GH105A and *Ps*GH105B was tested using 1 mM large unsaturated oligosaccharides as the substrate in 50 mM Tris (pH 7.5) with 150 mM NaCl. Reactions were initiated by simultaneous addition of *Ye*KdgF and/or a single *Ps*GH105, each to a final concentration of 1 μM. No-enzyme control reaction mixtures contained binding buffer or 20 mM Tris (pH 8.0) in place of enzyme. The preparation of *Ye*KdgF was confirmed to be active by testing it against $\Delta GalUA_2$ in a linked assay with $GalUA_2$ and *Ye*OgI as described previously (16).

Galacturonate release assay. Liberation of free GalUA from PGA or saturated oligosaccharides by *Ps*GH28 was observed in real time using the Megazyme D-glucuronic/D-galacturonic acid assay kit according to the manufacturer's instructions. Reaction mixtures contained 0.5% (wt/vol) PGA, or 1 mM $GalUA_2$ or $GalUA_3$, and 150 mM NaCl in kit buffer, and reactions were initiated by the addition of *Ps*GH28 to 1 μM. Data were processed according to the manufacturer's instructions and corrected for background changes in absorbance observed when binding buffer was added in place of *Ps*GH28.

***In vitro* reconstitution of enzyme pathway.** The rates of GalUA and DKI production from pectin by the complete set of PS47 pectinases and the effect of omitting one or more enzymes were determined using enzyme-coupled assays. GalUA release was quantified using the Megazyme D-glucuronic/D-galacturonic acid assay kit, according to the manufacturer's instructions. In addition to the standard kit components, reaction mixtures contained each pectinase at 1 μM and 150 mM NaCl. Reactions were initiated by the addition of citrus pectin to a final concentration of 0.2% (wt/vol), and OD_{340} readings were taken every 5 to 20 seconds. DKI release was quantified using the isomerase *Ye*KduI and dehydrogenase *Ye*KduD as previously described (16). Reaction mixtures contained 1 mM NADH, 150 mM NaCl, 50 mM Tris (pH 7.5), and 1 μM all enzymes, including *Ye*KduI and *Ye*KduD. As for GalUA release, reactions were initiated by the addition of citrus pectin to a final concentration of 0.2% (wt/vol), and OD_{340} readings were taken. For both coupled assays, initial rates were determined, blanked using the no-enzyme control, and converted into μM/min using either the manufacturer's instructions (for GalUA) or an extinction coefficient of 6,220 M^{-1} cm^{-1} (for DKI).

Carbohydrate binding assays. The binding of the DUF of *Ps*GH105A to PGA and $\Delta GalUA_{\geq n=4}$ was evaluated using differential scanning fluorimetry. Samples contained DUF at 1 mg/ml, 10× SYPRO Orange (Invitrogen, Carlsbad, CA), 500 mM NaCl, 20 mM buffer (MES [pH 5.7 and 6.5], HEPES [pH 7.5], Tris-HCl [pH 8.0], or Tris-phosphate [pH 9.0]), and 0.1 or 0.2% PGA or $\Delta GalUA_{\geq n=4}$. Reaction mixtures were incubated in a Bio-Rad CFX96 Touch real-time PCR machine at 25 to 95°C with a ramp rate of 1°C/min and read using the HEX channel. Controls included samples of DUF to which dH_2O was added in place of ligand or binding buffer was added in place of DUF.

Accession number(s). The complete sequence of the *Pseudoalteromonas* sp. PS47 pectin PUL has been submitted to GenBank under accession number MH687413.

SUPPLEMENTAL MATERIAL

Supplemental material for this article may be found at https://doi.org/10.1128/AEM.02114-18.

SUPPLEMENTAL FILE 1, PDF file, 0.3 MB.

ACKNOWLEDGMENT

This research was supported by a Natural Sciences and Engineering Research Council of Canada Discovery grant (FRN 04355).

REFERENCES

1. Barbeyron T, Thomas F, Barbe V, Teeling H, Schenowitz C, Dossat C, Goesmann A, Leblanc C, Oliver Glöckner F, Czjzek M, Amann R, Michel G. 2016. Habitat and taxon as driving forces of carbohydrate catabolism in marine heterotrophic bacteria: example of the model algae-associated bacterium *Zobellia galactanivorans* Dsij^T. Environ Microbiol 18:4610–4627. https://doi.org/10.1111/1462-2920.13584.
2. Grondin JM, Tamura K, Déjean G, Abbott DW, Brumer H. 2017. Polysaccharide utilization loci: fueling microbial communities. J Bacteriol 199:e860-16.
3. Hemsworth GR, Dejean G, Davies GJ, Brumer H. 2016. Learning from microbial strategies for polysaccharide degradation. Biochem Soc Trans 44:94–108. https://doi.org/10.1042/BST20150180.
4. Voragen AGJ, Coenen G-J, Verhoef RP, Schols HA. 2009. Pectin, a versatile polysaccharide present in plant cell walls. Struct Chem 20:263–275. https://doi.org/10.1007/s11224-009-9442-z.
5. Chung D, Pattathil S, Biswal AK, Hahn MG, Mohnen D, Westpheling J. 2014. Deletion of a gene cluster encoding pectin degrading enzymes in *Caldicellulosiruptor bescii* reveals an important role for pectin in plant biomass recalcitrance. Biotechnol Biofuels 7:147. https://doi.org/10.1186/s13068-014-0147-1.
6. Shevchik VE, Condemine G, Robert-Baudouy J, Hugouvieux-Cotte-Pattat N. 1999. The exopolygalacturonate lyase PelW and the oligogalacturonate lyase Ogl, two cytoplasmic enzymes of pectin catabolism in *Erwinia chrysanthemi* 3937. J Bacteriol 181:3912–3919.
7. Ndeh D, Rogowski A, Cartmell A, Luis AS, Baslé A, Gray J, Venditto I, Briggs J, Zhang X, Labourel A, Terrapon N, Buffetto F, Nepogodiev S, Xiao Y, Field RA, Zhu Y, O'Neill MA, Urbanowicz BR, York WS, Davies GJ, Abbott DW, Ralet M-C, Martens EC, Henrissat B, Gilbert HJ. 2017. Complex pectin metabolism by gut bacteria reveals novel catalytic functions. Nature 544:65–70. https://doi.org/10.1038/nature21725.
8. Ridley BL, O'Neill MA, Mohnen D. 2001. Pectins: structure, biosynthesis, and oligogalacturonide-related signaling. Phytochemistry 57:929–967. https://doi.org/10.1016/S0031-9422(01)00113-3.
9. Schink B, Ward JC, Zeikus JG. 1981. Microbiology of wetwood: importance of pectin degradation and clostridium species in living trees. Appl Environ Microbiol 42:526–532.
10. Benoit I, Coutinho PM, Schols HA, Gerlach JP, Henrissat B, de Vries RP. 2012. Degradation of different pectins by fungi: correlations and contrasts between the pectinolytic enzyme sets identified in genomes and the growth on pectins of different origin. BMC Genomics 13:321. https://doi.org/10.1186/1471-2164-13-321.
11. Tayi L, Maku RV, Patel HK, Sonti RV. 2016. Identification of pectin degrading enzymes secreted by *Xanthomonas oryzae pv. oryzae* and determination of their role in virulence on rice. PLoS One 11:e0166396. https://doi.org/10.1371/journal.pone.0166396.
12. Despres J, Forano E, Lepercq P, Comtet-Marre S, Jubelin G, Yeoman CJ, Miller MEB, Fields CJ, Terrapon N, Le Bourvellec C, Renard CMGC, Henrissat B, White BA, Mosoni P. 2016. Unraveling the pectinolytic function of Bacteroides xylanisolvens using a RNA-seq approach and mutagenesis. BMC Genomics 17:147. https://doi.org/10.1186/s12864-016-2472-1.
13. Abbott DW, Boraston AB. 2008. Structural biology of pectin degradation by Enterobacteriaceae. Microbiol Mol Biol Rev 72:301–316. https://doi.org/10.1128/MMBR.00038-07.
14. Preiss J, Ashwell G. 1963. Polygalacturonic acid metabolism in bacteria. I. Enzymatic formation of 4-deoxy-L-threo-5-hexoseulose uronic acid. J Biol Chem 238:1571–1583.
15. Preiss J, Ashwell G. 1963. Polygalacturonic acid metabolism in bacteria. II. Formation and metabolism of 3-deoxy-D-glycero-2, 5-hexodiulosonic acid. J Biol Chem 238:1577–1583.
16. Hobbs JK, Lee SM, Robb M, Hof F, Barr C, Abe KT, Hehemann J-H, McLean R, Abbott DW, Boraston AB. 2016. KdgF, the missing link in the microbial metabolism of uronate sugars from pectin and alginate. Proc Natl Acad Sci U S A 113:6188–6193. https://doi.org/10.1073/pnas.1524214113.
17. Abbott DW, Gilbert HJ, Boraston AB. 2010. The active site of oligogalacturonate lyase provides unique insights into cytoplasmic oligogalacturonate β-elimination. J Biol Chem 285:39029–39038. https://doi.org/10.1074/jbc.M110.153981.
18. Condemine G, Robert-Baudouy J. 1991. Analysis of an *Erwinia chrysanthemi* gene cluster involved in pectin degradation. Mol Microbiol 5:2191–2202. https://doi.org/10.1111/j.1365-2958.1991.tb02149.x.
19. Condemine G, Hugouvieux-Cotte-Pattat N, Robert-Baudouy J. 1986. Isolation of *Erwinia chrysanthemi kduD* mutants altered in pectin degradation. J Bacteriol 165:937–941. https://doi.org/10.1128/jb.165.3.937-941.1986.
20. Hugouvieux-Cotte-Pattat N, Robert-Baudouy J. 1987. Hexuronate catabolism in *Erwinia chrysanthemi*. J Bacteriol 169:1223–1231. https://doi.org/10.1128/jb.169.3.1223-1231.1987.
21. Itoh T, Ochiai A, Mikami B, Hashimoto W, Murata K. 2006. A novel glycoside hydrolase family 105: the structure of family 105 unsaturated rhamnogalacturonyl hydrolase complexed with a disaccharide in comparison with family 88 enzyme complexed with the disaccharide. J Mol Biol 360:573–585. https://doi.org/10.1016/j.jmb.2006.04.047.
22. Collén PN, Jeudy A, Sassi J-F, Groisillier A, Czjzek M, Coutinho PM, Helbert W. 2014. A novel unsaturated β-glucuronyl hydrolase involved in ulvan degradation unveils the versatility of stereochemistry requirements in family GH105. J Biol Chem 289:6199–6211. https://doi.org/10.1074/jbc.M113.537480.
23. Jongkees SAK, Yoo H, Withers SG. 2014. Mechanistic investigations of unsaturated glucuronyl hydrolase from *Clostridium perfringens*. J Biol Chem 289:11385–11395. https://doi.org/10.1074/jbc.M113.545293.
24. Jongkees SAK, Withers SG. 2011. Glycoside cleavage by a new mechanism in unsaturated glucuronyl hydrolases. J Am Chem Soc 133. https://doi.org/10.1021/ja209067v.
25. Luis AS, Briggs J, Zhang X, Farnell B, Ndeh D, Labourel A, Baslé A, Cartmell A, Terrapon N, Stott K, Lowe EC, McLean R, Shearer K, Schückel J, Venditto I, Ralet M-C, Henrissat B, Martens EC, Mosimann SC, Abbott DW, Gilbert HJ. 2018. Dietary pectic glycans are degraded by coordinated enzyme pathways in human colonic Bacteroides. Nat Microbiol 3:210–219. https://doi.org/10.1038/s41564-017-0079-1.
26. Ensor L, Stosz S, Weiner R. 1999. Expression of multiple complex polysaccharide-degrading enzyme systems by marine bacterium strain 2-40. J Ind Microbiol Biotechnol 23:123–126. https://doi.org/10.1038/sj.jim.2900696.
27. Truong LV, Tuyen H, Helmke E, Binh LT, Schweder T. 2001. Cloning of two pectate lyase genes from the marine Antarctic bacterium *Pseudoalteromonas haloplanktis* strain ANT/505 and characterization of the enzymes. Extremophiles 5:35–44. https://doi.org/10.1007/s007920000170.
28. Ramaiah N, Chandramohan D. 1992. Densities, cellulases, alginate and pectin lyases of luminous and other heterotrophic bacteria associated with marine algae. Aquat Bot 44:71–81. https://doi.org/10.1016/0304-3770(92)90082-T.
29. Tang K, Lin Y, Han Y, Jiao N. 2017. Characterization of potential polysaccharide utilization systems in the marine Bacteroidetes *Gramella Flava* JLT2011 using a multi-omics approach. Front Microbiol 8:220. https://doi.org/10.3389/fmicb.2017.00220.
30. Imran M, Pant P, Shanbhag YP, Sawant SV, Ghadi SC. 2017. Genome aequence of *Microbulbifer mangrovi* DD-13T reveals its versatility to degrade multiple polysaccharides. Mar Biotechnol 19:116–124. https://doi.org/10.1007/s10126-017-9737-9.
31. Hehemann J-H, Truong L, Van Unfried F, Welsch N, Kabisch J, Heiden SE, Junker S, Becher D, Thürmer A, Daniel R, Amann R, Schweder T. 2017. Aquatic adaptation of a laterally acquired pectin degradation pathway in marine gammaproteobacteria. Environ Microbiol 19:2320–2333. https://doi.org/10.1111/1462-2920.13726.
32. Desikachary TV, Dweltz NE. 1961. The chemical composition of the diatom frustule. Proc Indian Acad Sci Sect B 53:157–165.
33. Ovodova RG, Vaskovsky VE, Ovodov YS. 1968. The pectic substances of

zosteraceae. Carbohydr Res 6:328–332. https://doi.org/10.1016/S0008-6215(00)81454-8.
34. Gloaguen V, Brudieux V, Closs B, Barbat A, Krausz P, Sainte-Catherine O, Kraemer M, Maes E, Guerardel Y. 2010. Structural characterization and cytotoxic properties of an apiose-rich pectic polysaccharide obtained from the cell wall of the marine phanerogam *Zostera marina*. J Nat Prod 73:1087–1092. https://doi.org/10.1021/np100092c.
35. Lv Y, Shan X, Zhao X, Cai C, Zhao X, Lang Y, Zhu H, Yu G. 2015. Extraction, isolation, structural characterization and anti-tumor properties of an apigalacturonan-rich polysaccharide from the sea grass *Zostera caespitosa* Miki. Mar Drugs 13:3710–3731. https://doi.org/10.3390/md13063710.
36. Khotimchenko Y, Khozhaenko E, Kovalev V, Khotimchenko M. 2012. Cerium binding activity of pectins isolated from the seagrasses *Zostera marina* and *Phyllospadix iwatensis*. Mar Drugs 10:834–848. https://doi.org/10.3390/md10040834.
37. Hettle AG, Vickers C, Robb CS, Liu F, Withers SG, Hehemann J-H, Boraston AB. 2018. The molecular basis of polysaccharide sulfatase activity and a nomenclature for catalytic subsites in this class of enzyme. Structure 26:747–758.e4. https://doi.org/10.1016/j.str.2018.03.012.
38. Zhang H, Yohe T, Huang L, Entwistle S, Wu P, Yang Z, Busk PK, Xu Y, Yin Y. 2018. dbCAN2: a meta server for automated carbohydrate-active enzyme annotation. Nucleic Acids Res 46:W95–W101. https://doi.org/10.1093/nar/gky418.
39. Boratyn GM, Schäffer AA, Agarwala R, Altschul SF, Lipman DJ, Madden TL. 2012. Domain enhanced lookup time accelerated BLAST. Biol Direct 7:12. https://doi.org/10.1186/1745-6150-7-12.
40. Kelley LA, Mezulis S, Yates CM, Wass MN, Sternberg MJE. 2015. The Phyre2 web portal for protein modeling, prediction and analysis. Nat Protoc 10:845–858. https://doi.org/10.1038/nprot.2015.053.
41. Drozdetskiy A, Cole C, Procter J, Barton GJ. 2015. JPred4: a protein secondary structure prediction server. Nucleic Acids Res 43:W389–W394. https://doi.org/10.1093/nar/gkv332.
42. Lin K, Simossis VA, Taylor WR, Heringa J. 2005. A simple and fast secondary structure prediction method using hidden neural networks. Bioinformatics 21:152–159. https://doi.org/10.1093/bioinformatics/bth487.
43. Buchan DWA, Minneci F, Nugent TCO, Bryson K, Jones DT. 2013. Scalable web services for the PSIPRED Protein Analysis Workbench. Nucleic Acids Res 41:W349–W357. https://doi.org/10.1093/nar/gkt381.
44. Condemine G, Hugouvieux-Cotte-Pattat N, Robert-Baudouy J. 1984. An enzyme in the pectinolytic pathway of *Erwinia chrysanthemi*: 2-keto-3-deoxygluconate oxidoreductase. Microbiology 130:2839–2844. https://doi.org/10.1099/00221287-130-11-2839.
45. Maeda M, Koshikawa M, Nisizawa K, Takano K. 1966. Cell wall constituents, especially pectic substance of a marine phanerogam *Zostera marina*. Shokubutsugaku Zasshi 79:422–426. https://doi.org/10.15281/jplantres1887.79.422.
46. Tang K, Jiao N, Liu K, Zhang Y, Li S. 2012. Distribution and functions of TonB-dependent transporters in marine bacteria and environments: implications for dissolved organic matter utilization. PLoS One 7:e41204. https://doi.org/10.1371/journal.pone.0041204.
47. Blanvillain S, Meyer D, Boulanger A, Lautier M, Guynet C, Denancé N, Vasse J, Lauber E, Arlat M. 2007. Plant carbohydrate scavenging through TonB-dependent receptors: a feature shared by phytopathogenic and aquatic bacteria. PLoS One 2:e224. https://doi.org/10.1371/journal.pone.0000224.
48. Juncker AS, Willenbrock H, von Heijne G, Brunak S, Nielsen H, Krogh A. 2003. Prediction of lipoprotein signal peptides in Gram-negative bacteria. Protein Sci 12:1652–1662. https://doi.org/10.1110/ps.0303703.
49. Nielsen H. 2017. Predicting secretory proteins with SignalP. Methods Mol Biol 1611:59–73. https://doi.org/10.1007/978-1-4939-7015-5_6.
50. Mulligan C, Fischer M, Thomas GH. 2011. Tripartite ATP-independent periplasmic (TRAP) transporters in bacteria and archaea. FEMS Microbiol Rev 35:68–86. https://doi.org/10.1111/j.1574-6976.2010.00236.x.
51. Zhao J, Binns AN. 2016. Involvement of *Agrobacterium tumefaciens* galacturonate tripartite ATP-independent periplasmic (TRAP) transporter GaaPQM in virulence gene expression. Appl Environ Microbiol 82:1136–1146. https://doi.org/10.1128/AEM.02891-15.
52. Abbott DW, Boraston AB. 2007. Specific recognition of saturated and 4,5-unsaturated hexuronate sugars by a periplasmic binding protein involved in pectin catabolism. J Mol Biol 369:759–770. https://doi.org/10.1016/j.jmb.2007.03.045.
53. Shibaeva VI, Ovodova RG, Ovodov YS. 1971. Pectin substances of seaweeds. VII. Acetolysis of zosterin. Chem Nat Compd 7:240–242. https://doi.org/10.1007/BF00568987.
54. Schmidt US, Koch L, Rentschler C, Kurz T, Endreß HU, Schuchmann HP. 2015. Effect of molecular weight reduction, acetylation and esterification on the emulsification properties of citrus pectin. Food Biophys 10:217–227. https://doi.org/10.1007/s11483-014-9380-1.
55. Edwards MC, Doran-Peterson J. 2012. Pectin-rich biomass as feedstock for fuel ethanol production. Appl Microbiol Biotechnol 95:565–575. https://doi.org/10.1007/s00253-012-4173-2.
56. Doran JB, Cripe J, Sutton M, Foster B. 2000. Fermentations of pectin-rich biomass with recombinant bacteria to produce fuel ethanol. Appl Biochem Biotechnol 84-86:141–152. https://doi.org/10.1385/ABAB:84-86:1-9:141.
57. Therkildsen M, Isaksen M, Lomstein B. 1997. Urea production by the marine bacteria *Delaya venusta* and *Pseudomonas stutzeri* grown in a minimal medium. Aquat Microb Ecol 13:213–217. https://doi.org/10.3354/ame013213.
58. Robb M, Hobbs JK, Boraston AB. 2017. Separation and visualization of glycans by fluorophore-assisted carbohydrate electrophoresis. Methods Mol Biol 1588:215–221. https://doi.org/10.1007/978-1-4939-6899-2_17.
59. Grsic-Rausch S, Rausch T. 2004. A coupled spectrophotometric enzyme assay for the determination of pectin methylesterase activity and its inhibition by proteinaceous inhibitors. Anal Biochem 333:14–18. https://doi.org/10.1016/j.ab.2004.04.042.